cmgh
CELLULAR AND MOLECULAR GASTROENTEROLOGY AND HEPATOLOGY

ORIGINAL RESEARCH

The Ninj1/Dusp1 Axis Contributes to Liver Ischemia Reperfusion Injury by Regulating Macrophage Activation and Neutrophil Infiltration

Yuanchang Hu,[1,2,*] Feng Zhan,[3,*] Yong Wang,[1,2,*] Dong Wang,[1,2] Hao Lu,[1,2] Chen Wu,[1,2] Yongxiang Xia,[1,2] Lijuan Meng,[4] Feng Zhang,[1,2] Xun Wang,[1,2] and Shun Zhou[1,2]

[1]Hepatobiliary Center, The First Affiliated Hospital of Nanjing Medical University, Nanjing, China; [2]Key Laboratory of Liver Transplantation, Chinese Academy of Medical Sciences, Nanjing, China; [3]Department of Hepatobiliary and Laparoscopic Surgery, The Affiliated Yixing Hospital, Jiangsu University, Yixing, China; and [4]Department of Geriatric Oncology, The First Affiliated Hospital, Nanjing Medical University, Nanjing, China

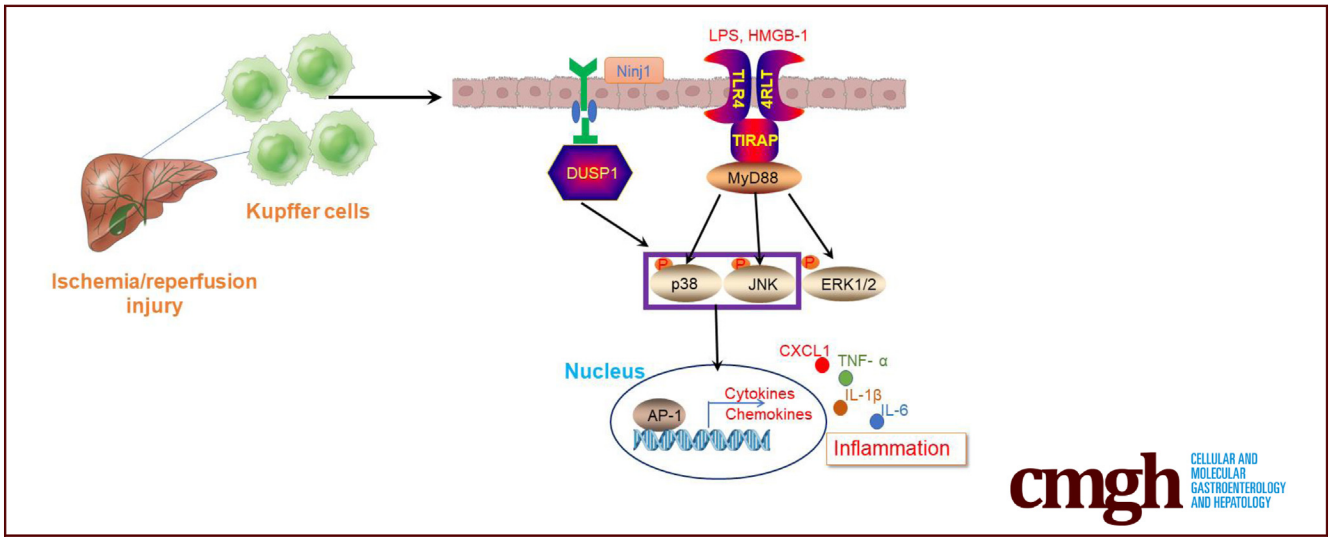

SUMMARY

Nerve injury–induced protein 1 plays an important role in regulating innate immune response under inflammatory conditions. Here, we report that nerve injury–induced protein 1–dual specificity phosphatase 1 signaling modulates the proinflammatory response of Kupffer cells and influences neutrophil infiltration during liver ischemia and reperfusion injury.

BACKGROUND & AIMS: Liver ischemia-reperfusion (IR) injury represents a major risk factor in both partial hepatectomy and liver transplantation. Nerve injury–induced protein 1 (Ninj1) is widely recognized as an adhesion molecule in leukocyte trafficking under inflammatory conditions, but its role in regulating sterile inflammation during liver IR injury remains unclear.

METHODS: Myeloid Ninj1-deficient mice were generated by bone marrow chimeric models using Ninj1 knockout mice and wild-type mice. In vivo, a liver partial warm ischemia model was applied. Liver injury and hepatic inflammation were investigated. In vitro, primary Kupffer cells (KCs) isolated from Ninj1 knockout and wild-type mice were used to explore the function and mechanism of Ninj1 in modulating KC inflammation upon lipopolysaccharide stimulation.

RESULTS: Ninj1 deficiency in KCs protected mice against liver IR injury during the later phase of reperfusion, especially in neutrophil infiltration, intrahepatic inflammation, and hepatocyte apoptosis. This prompted ischemia-primed KCs to decrease proinflammatory cytokine production. In vitro and in vivo, using small-interfering RNA against dual-specificity phosphatase 1 (DUSP1), we found that Ninj1 deficiency diminished the inflammatory response in KCs and neutrophil infiltration through DUSP1-dependent deactivation of the c-Jun-N-terminal kinase and p38 pathways. Sivelestat, a neutrophil elastase inhibitor, functioned similarly to Ninj1 deficiency, resulting in both mitigated hepatic IR injury in mice and a more rapid recovery of liver function in patients undergoing liver resection.

CONCLUSIONS: The Ninj1/Dusp1 axis contributes to liver IR injury by regulating the proinflammatory response of KCs, and influences neutrophil infiltration, partly by subsequent regulation of C-X-C motif chemokine ligand 1 (CXCL1) production after IR. *(Cell Mol Gastroenterol Hepatol 2023;15:1071–1084; https://doi.org/10.1016/j.jcmgh.2023.01.008)*

Keywords: Liver IR Injury; Kupffer Cells; Nerve Injury-Induced Protein 1; Dual-Specificity Phosphatase 1; Sterile Inflammation.

Liver ischemia-reperfusion (IR) injury remains a major cause of liver failure or dysfunction after liver transplantation and resection. Although the pathogenesis of liver IR injury is very complex, it involves 2 major phases: hepatocellular injury and death as a result of deprivation of oxygen and nutrients, and subsequent sterile inflammatory insult caused by the activation and recruitment of macrophages and neutrophils. Activation of liver-resident macrophages (Kupffer cells [KCs]) by damage-associated molecular pattern molecules, which are released by injured or dead hepatocytes, is considered the initial response to sterile inflammation. Activated KCs secrete cytokines to prime intrahepatic inflammation and release chemokines to recruit peripheral blood mononuclear cells, such as macrophages and neutrophils, into the necrotic region, resulting in amplification of intrahepatic inflammation.

Nerve injury–induced protein 1 (Ninjurin-1 [Ninj1]) is a cell-surface protein with 2 transmembrane regions. It originally was reported to be up-regulated in neurons and Schwann cells after nerve injury, and is related to nerve regeneration.[1] Ninj1 is a well-known adhesion molecule and is expressed widely in several tissues and cells, including myeloid cells, endothelial cells, neurons, and cancer cells.[2–4] An increasing body of evidence suggests that Ninj1 plays an important role in various inflammatory processes by regulating leukocyte infiltration.

Ninj1 blockade decreases the infiltration of macrophages, dendritic cells, and antigen-presenting cells into the central nervous system and improves the clinical signs of experimental allergic encephalomyelitis (EAE).[5] In a study using Ninj1 knockout (KO) mice, Ninj1 deficiency was found to attenuate EAE susceptibility, with reduced leukocyte infiltration and decreased adherence of leukocytes to retinal vessels in endotoxin-induced uveitis mice.[6] In addition to nervous system inflammation, Ninj1 is involved in various inflammatory diseases in other organs. For instance, in systemic sepsis, Ninj1 activation promotes leukocyte migration and regulates Toll-like receptor 4 (TLR4) signaling via p38 and Activator protein 1 (AP-1).[7] Ninj1 also regulates macrophage M1/M2 polarization and induces microbial imbalance during colitis development.[8] Activation of Ninj1 in macrophages results in increased cytokine and chemokine secretion with exacerbation of experimental colitis.[9]

Sterile inflammation plays a crucial role in the pathophysiology of organ IR injury.[10] A recent study reported that Ninj1 is dynamically expressed in different immune cells at different times after transient focal cerebral ischemia, suggesting the critical role of Ninj1 in modulating ischemia-induced sterile inflammation.[11] Indeed, a subsequent study by the same team reported that Ninj1-mediated neutrophil infiltration is responsible for inflammation and brain damage postischemia.[12] Because many innate immune cells reside in the liver, the role of Ninj1 expressed by these cells in regulating IR-induced sterile inflammation and modulating liver IR injury remains unclear.

Therefore, in the present study, bone marrow chimeric mice were established to investigate whether and how Ninj1 in KCs modulates the intrahepatic inflammatory response upon liver IR stress. Briefly, we examined whether proinflammatory cytokine secretion and neutrophil infiltration was affected in Ninj1-deficient KCs, along with their effect on intrahepatic inflammation and liver injury post-IR.

Results

Ninj1 Activation in KCs Promoted Liver IR Injury at a Later Time

First, we evaluated Ninj1 expression in both hepatocytes and KCs of IR-induced wild-type (WT) livers. As shown in Figure 1*A*, compared with the sham group, Ninj1 was up-regulated slightly in hepatocytes after 6 hours of reperfusion, whereas its levels were increased markedly in KCs, suggesting that Ninj1 activation in KCs may play a more important role in modulating liver IR injury. Thus, bone marrow chimeric mice were generated to investigate the role of Ninj1 in hepatic macrophages after IR injury. WT→WT and KO→WT mice were subjected to 90 minutes of warm ischemia or a sham procedure, and liver tissues and blood specimens were collected at 6 or 24 hours after reperfusion. Western blot analysis showed that Ninj1 was activated significantly in KCs isolated from WT→WT mice post-IR, whereas it could not be detected in KCs of KO→WT mice post-IR (Figure 1*B*). However, there was no difference in Ninj1 expression in hepatocytes in the 2 groups, indicating that Ninj1 was deleted in KCs but not in hepatocytes in KO→WT mice (Figure 1*C*).

Then, we evaluated live damage in different groups of mice. Interestingly, although initial liver injury after 6 hours of reperfusion was comparable between KO→WT and WT→WT mice, liver damage at a later time point (24 hours after reperfusion) was alleviated significantly in KO→WT mice compared with that in WT→WT mice, as evidenced by a smaller necrotic area and lower Suzuki scores (Figure 1*D*–*F*). Consistent with the histologic architecture, liver function evaluated by alanine aminotransferase (ALT) and aspartate aminotransferase (AST) levels was highly preserved in KO→WT mice at 24 hours post-IR, whereas no significant difference was observed between the 2 groups at 6 hours post-IR (Figure 1*G* and *H*). These results indicate

***Authors share co-first authorship.**

Abbreviations used in this paper: **ALT, alanine aminotransferase; ASK1, apoptosis signal-regulating kinase 1; AST, aspartate aminotransferase; Bax, Bcl2-associated x; Bcl-2, B-cell lymphoma 2; CCL, C-C motif chemokine ligand; CXCL, C-X-C motif chemokine ligand; DUSP1, dual-specificity phosphatase 1; EAE, experimental allergic encephalomyelitis; ERK, extracellular signal–regulated kinase; IL, interleukin; IR, ischemia-reperfusion; JNK, c-Jun-N-terminal kinase; KC, Kupffer cell; KO, knock out; LPS, lipopolysaccharide; MAPK, mitogen-activated protein kinase; MPO, myeloperoxidase; mRNA, messenger RNA; MyD88, myeloid differentiation primary response 88; Ninj1, nerve injury-induced protein 1; NS-siRNA, nonspecific small interfering RNA; p-ASK1, phosphorylated-ASK1; p-JNK, phosphorylated-JNK; p-p38, phosphorylated-p38; p-TAK1, phosphorylated-TAK1; siRNA, small interfering RNA; TAK1, transforming growth factor-β–activated kinase 1; TLR4, Toll-like receptor 4; TNF-α, tumor necrosis factor-α; TRIF, TIR-domain–containing adapter–inducing interferon-β; TUNEL, terminal deoxynucleotidyl transferase–mediated deoxyuridine triphosphate nick-end labeling; WT, wild-type.**

Most current article

2352-345X
https://doi.org/10.1016/j.jcmgh.2023.01.008

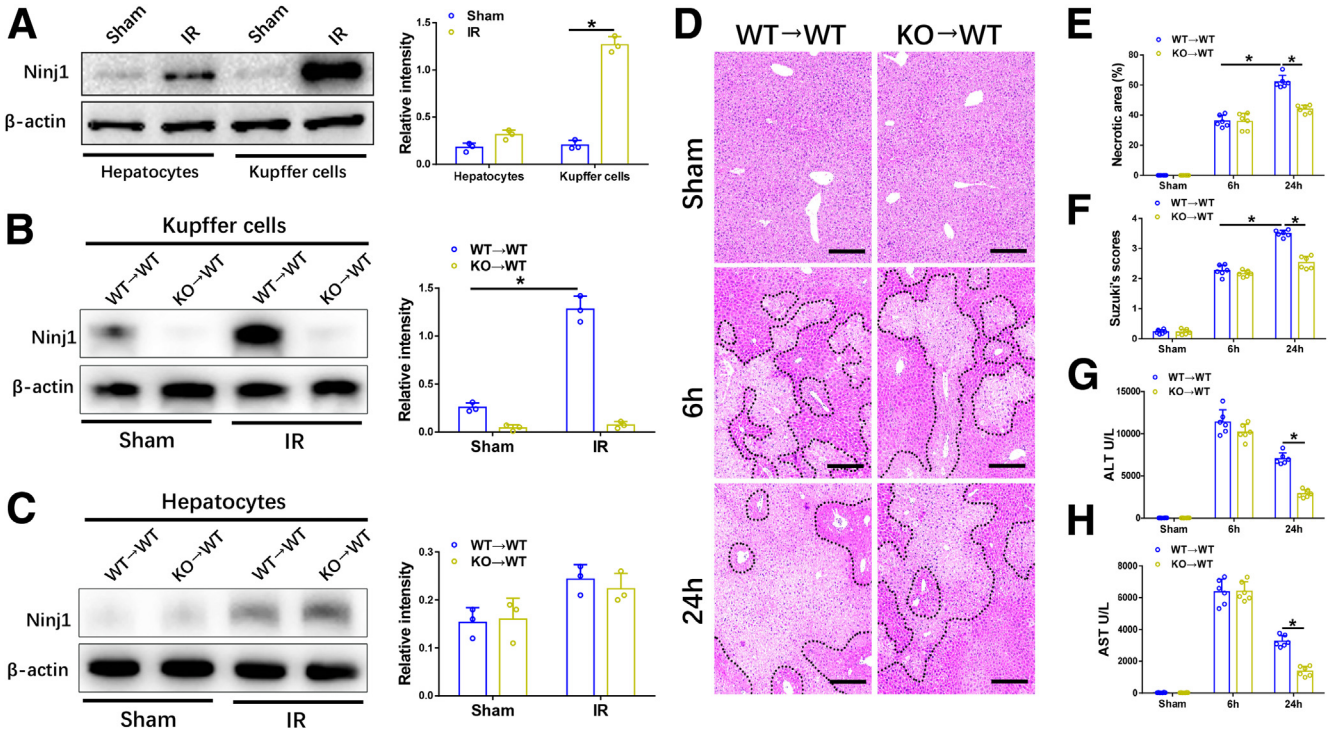

Figure 1. Ninj1 activation in KCs promoted liver IR injury at a later time. WT mice were subjected to 90 minutes of partial warm liver ischemia, followed by 6 hours of reperfusion. Primary hepatocytes and KCs were isolated from livers of the sham and IR groups. (*A*) Western blot analysis of Ninj1 and β-actin expression in hepatocytes and KCs. Relative intensity analyzed by ImageJ software (National Institutes of Health). Chimeric mice were established as described in the Materials and Methods section. WT→WT and KO→WT mice were subjected to 90 minutes of warm ischemia or a sham procedure, and liver tissues and blood specimens were collected at 6 or 24 hours after reperfusion. (*B* and *C*) Western blot analysis of Ninj1 and β-actin expression in hepatocytes and KCs. Relative intensity analyzed by ImageJ software. (*D*) Representative H&E staining of ischemic livers from each group for different times. *Scale bar*: 100 μm. (*E*) Necrotic areas in ischemic livers analyzed by ImageJ software. (*F*) Suzuki histologic grading of IR injury. (*G* and *H*) Serum levels of ALT and AST. All results are representative of at least 2 independent experiments; n = 6 mice/group. $^*P < .05$. All data are presented as the means ± SD.

that Ninj1 deficiency in KCs protects mice against liver IR injury during the later phase of reperfusion.

Ninj1 Deficiency in KCs Decreased Hepatocyte Apoptosis During a Later Phase Post-IR

Oxidative stress and subsequent inflammatory responses are the 2 major causes of IR-induced hepatocyte apoptosis. Therefore, we determined whether Ninj1 deficiency in KCs can prevent IR-induced hepatocyte apoptosis. As shown in Figure 2*A* and *B*, similar numbers of terminal deoxynucleotidyl transferase–mediated deoxyuridine triphosphate nick-end labeling (TUNEL)-positive hepatocytes were observed in the WT→WT and KO→WT livers 6 hours after reperfusion, whereas the number of TUNEL-positive hepatocytes in the KO→WT livers 24 hours after reperfusion was much lower than that in WT→WT livers. Furthermore, the messenger RNA (mRNA) levels of apoptosis-related molecules, including B-cell lymphoma 2 (Bcl-2) and Bcl2-associated x (BAX), were comparable between the 2 groups at 6 hours post-IR. However, the gene induction of Bcl-2 was increased and that of Bax was decreased in KO→WT livers at 24 hours post-IR, compared with those in WT→WT livers (Figure 2*C* and *D*). Western blot analysis showed comparable protein levels of Bcl-2, Bax, and cleaved caspase-3 between the 2 groups at 6 hours post-IR, while KO→WT mice showed increased expression of Bcl-2 and decreased expression of Bax and cleaved caspase-3 compared with WT→WT mice at 24 hours post-IR (Figure 2*E*). These observations show that Ninj1 deficiency in KCs prevents IR-induced hepatocyte apoptosis during the later phase.

Ninj1 Deficiency in KCs Restrained Neutrophil but Not Macrophage Infiltration, and Inhibited Intrahepatic Inflammation Post-IR

Intrahepatic infiltration of circulating monocytes during reperfusion amplifies IR-induced inflammatory injury. We examined whether Ninj1 regulates macrophage and neutrophil recruitment post-IR. Immunohistochemical staining results showed that compared with WT→WT mice, KO→WT mice showed significantly decreased intrahepatic neutrophil infiltration at 6 hours post-IR, whereas the number of infiltrated macrophages between the 2 groups was not different (Figure 3*A*–*D*). Furthermore, IR-stressed KO→WT livers showed lower proinflammatory gene induction (*IL6*, *IL1β*, and *TNF-α*) than that in IR-stressed

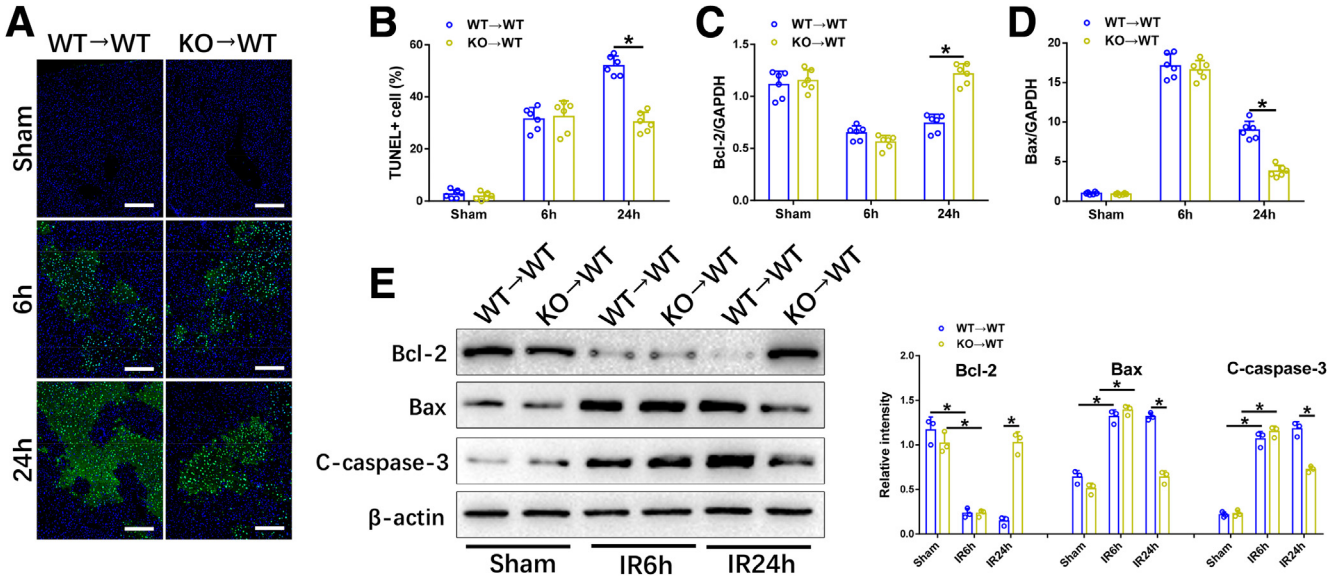

Figure 2. Ninj1 deficiency in KCs decreased hepatocyte apoptosis during the later phase post-IR. Chimeric mice were established as described in the Materials and Methods section. WT→WT and KO→WT mice were subjected to 90 minutes of warm ischemia or a sham procedure, and liver tissues and blood specimens were collected at 6 or 24 hours after reperfusion. (*A*) Immunofluorescence staining of TUNEL+ cells in ischemic livers from each group. *Scale bar*: 100 μm. (*B*) Quantification of TUNEL+ cells per high-power field. (*C* and *D*) Quantitative RT-PCR analysis of *Bcl-2* and *Bax* gene induction in livers from each group. (*E*) Western blot analysis of Bcl-2, Bax, C-caspase-3, and β-actin expression in livers from each group. Relative intensity analyzed by ImageJ software (National Institutes of Health). All results are representative of at least 2 independent experiments; n = 6 mice/group. *$P < .05$. All data are presented as the means ± SD. GAPDH, glyceraldehyde-3-phosphate dehydrogenase. C-caspase-3, Cleaved-caspase-3.

WT→WT livers (Figure 3*E*). The gene expression levels of C-X-C motif chemokine ligand (CXCL) 1 and CXCL2 (2 major neutrophil chemokines) were increased significantly in WT→WT and KO→WT livers in response to IR, whereas the increased levels were distinct between the 2 groups (Figure 3*E*). Liver tissue reverse-transcription polymerase chain reaction (RT-PCR) results indicated that IR-stressed KO→WT livers showed markedly decreased *CXCL1* expression but comparable *CXCL2* expression compared with that in IR-stressed WT→WT livers. As shown in Figure 3*F*, similar results were obtained for the serum levels of interleukin (IL)6, IL1β, tumor necrosis factor-α (TNF-α), CXCL1, and CXCL2. C-C motif chemokine ligand (CCL) family chemokines (CCL1, CCL2, CCL3, and CCL5) also were detected, the results showed no difference between the 2 groups post-IR (Figure 3*E* and *F*). These results suggest that Ninj1 deficiency in KCs inhibits intrahepatic inflammation and suppressed neutrophil infiltration after reperfusion, potentially because of reduced CXCL1 production.

Ninj1-Deficient KCs Were Responsible for Decreased Expression of Proinflammatory Cytokines and CXCL1 Both Ex Vivo and In Vitro

Because tissue-resident macrophages are the major source of inflammatory cytokines and chemokines, KCs isolated from IR-stressed KO→WT and WT→WT livers were subjected to ex vivo studies. In line with our in vivo results, KCs isolated from IR-stressed KO→WT livers showed decreased levels of proinflammatory cytokines (IL6, IL1β, and TNF-α) and CXCL1 at both the mRNA and protein levels, compared with those in KCs isolated from WT→WT livers (Figure 4*A* and *B*). To further confirm the role of Ninj1 in regulating inflammatory responses in vitro, KCs isolated from WT and Ninj1 KO mice were subjected to lipopolysaccharide (LPS) stimulation. Consistent with the ex vivo results, LPS-stressed Ninj1 KO KCs showed lower gene and protein levels of IL6, IL1β, TNF-α, and CXCL1, compared with those in LPS-stressed WT KCs (Figure 4*C* and *D*).

Ninj1 Deficiency Diminished the Inflammatory Response in KCs Through Dual Specificity Phosphatase 1–Dependent Deactivation of c-Jun-N-Terminal Kinase and p38 In Vitro

Upon LPS-induced TLR4 activation, CXCL2 synthesis in macrophages is regulated through the myeloid differentiation primary response 88 (MyD88), as well as the Toll/Interleukin-1 receptor-domain–containing adapter–inducing interferon-β (TRIF) pathway, whereas CXCL1 synthesis is restricted to the MyD88 pathway.[13] Therefore, we investigated whether reduced CXCL1 in Ninj1-deficient KCs was related to the TLR4/MyD88 pathway. However, Western blot analysis showed no obvious alteration in MyD88 activation in WT and Ninj1 KO KCs upon LPS stimulation (Figure 5*A*). Because mitogen-activated protein kinases (MAPKs) are critical players downstream of the TLR/MyD88 pathway, we examined the 3 canonical c-Jun-N-terminal kinase (JNK), extracellular signal–regulated kinase (ERK), and p38 pathways. Interestingly, phosphorylated-p38 (p-p38) and phosphorylated-JNK (p-JNK) were inhibited markedly in Ninj1 KO

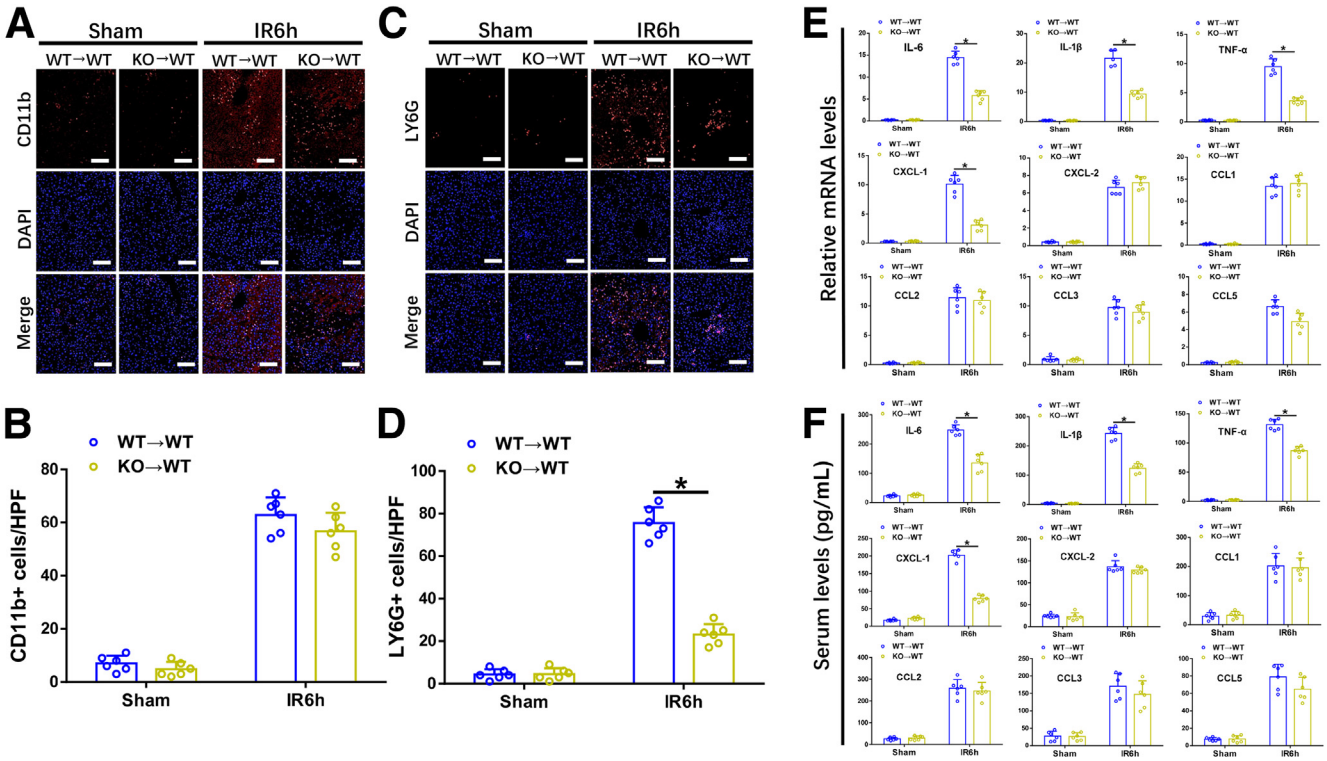

Figure 3. Ninj1 deficiency in KCs restrained neutrophils but not macrophage infiltration, and inhibited intrahepatic inflammation post-IR. Chimeric mice were established as described in the Materials and Methods section. WT→WT and KO→WT mice were subjected to 90 minutes of warm ischemia or a sham procedure, and liver tissues and blood specimens were collected at 24 hours after reperfusion. (*A* and *B*) Representative immunofluorescence staining of CD11b (red) and 4',6-diamidino-2-phenylindole dihydrochloride (DAPI) (blue) in livers from each group, quantification of CD11b+ cells per high-power field. *Scale bar*: 100 μm. (*C* and *D*) Representative immunofluorescence staining of LY6G (red) and DAPI (blue) in livers from each group, quantification of LY6G+ cells per high-power field. *Scale bar*: 100 μm. (*E*) Quantitative RT-PCR analysis of liver inflammatory cytokines and chemokine gene induction (*IL6*, *IL1β*, *TNF-α*, *CXCL-1*, *CXCL-2*, *CCL1*, *CCL2*, *CCL3*, and *CCL5*). (*F*) Enzyme-linked immunosorbent assay of inflammatory cytokine and chemokine levels in serum. All results are representative of at least 2 independent experiments; n = 6 mice/group. *$P < .05$. All data are presented as the means ± SD. LY6G, lymphocyte antigen 6 complex locus g.

KCs, with no significant effect on phosphorylated-ERK (p-ERK) (Figure 5*B*).

Studies have shown that phosphorylation of apoptosis signal-regulating kinase 1 (ASK1) and transforming growth factor-β–activated kinase 1 (TAK1) (2 members of the Mitogen-activated protein kinase kinase kinase family) are crucial for activating JNK and p38 cascades.[14–18] Dual-specificity phosphatase 1 (DUSP1), a MAPK phosphatase, also has been reported to deactivate JNK and p38 by dephosphorylating both tyrosine and threonine-phosphate residues.[19,20] Therefore, we examined the expression of phosphorylated-ASK1 (p-ASK1), phosphorylated-TAK1 (p-TAK1), and DUSP1 by Western blot. As shown in Figure 5*C*, LPS treatment strongly up-regulated Ninj1 in WT KCs, but not in KO KCs, while the expression of p-ASK1 and p-TAK1 was comparable between the 2 groups. Notably, LPS-stressed KO KCs showed much higher levels of DUSP1 than that in LPS-stressed WT KCs, suggesting that DUSP1 might be involved in Ninj1-mediated modulation of JNK and p38 pathways (Figure 5*C*).

To further determine whether repression of JNK and p38 in Ninj1 KO KCs is DUSP1-dependent, DUSP1-specific small interfering RNA (DUSP1-siRNA) was used to knockdown DUSP1 in both WT and Ninj1 KO KCs stimulated with LPS, with nonspecific siRNA (NS-siRNA) as a control. DUSP1 inhibition strongly activated JNK and p38, as indicated by increased levels of p-JNK and p-p38 in Ninj1 KO KCs, but no effects were found in WT KCs (Figure 5*D*). Furthermore, compared with NS-siRNA–treated KO KCs, DUSP1-siRNA treatment significantly enhanced the proinflammatory response, indicated by increased levels of IL6, IL1β, TNF-α, and CXCL1 (Figure 5*E* and *F*). These data indicate that Ninj1 deficiency blunts the inflammatory response in LPS-stressed KCs through DUSP1-mediated inactivation of JNK and p38 pathways.

Ninj1 Deficiency Attenuated IR-Induced Intrahepatic Inflammation and Neutrophil Infiltration by DUSP1-Dependent Inhibition of JNK and p38 Pathways In Vivo

To further explore DUSP1 involvement in Ninj1-mediated intrahepatic inflammation and neutrophil infiltration in response to IR, mannose-conjugated polymers were used to deliver DUSP1-siRNA or NS-siRNA specifically to phagocytes, before liver IR onset. DUSP1-siRNA treatment

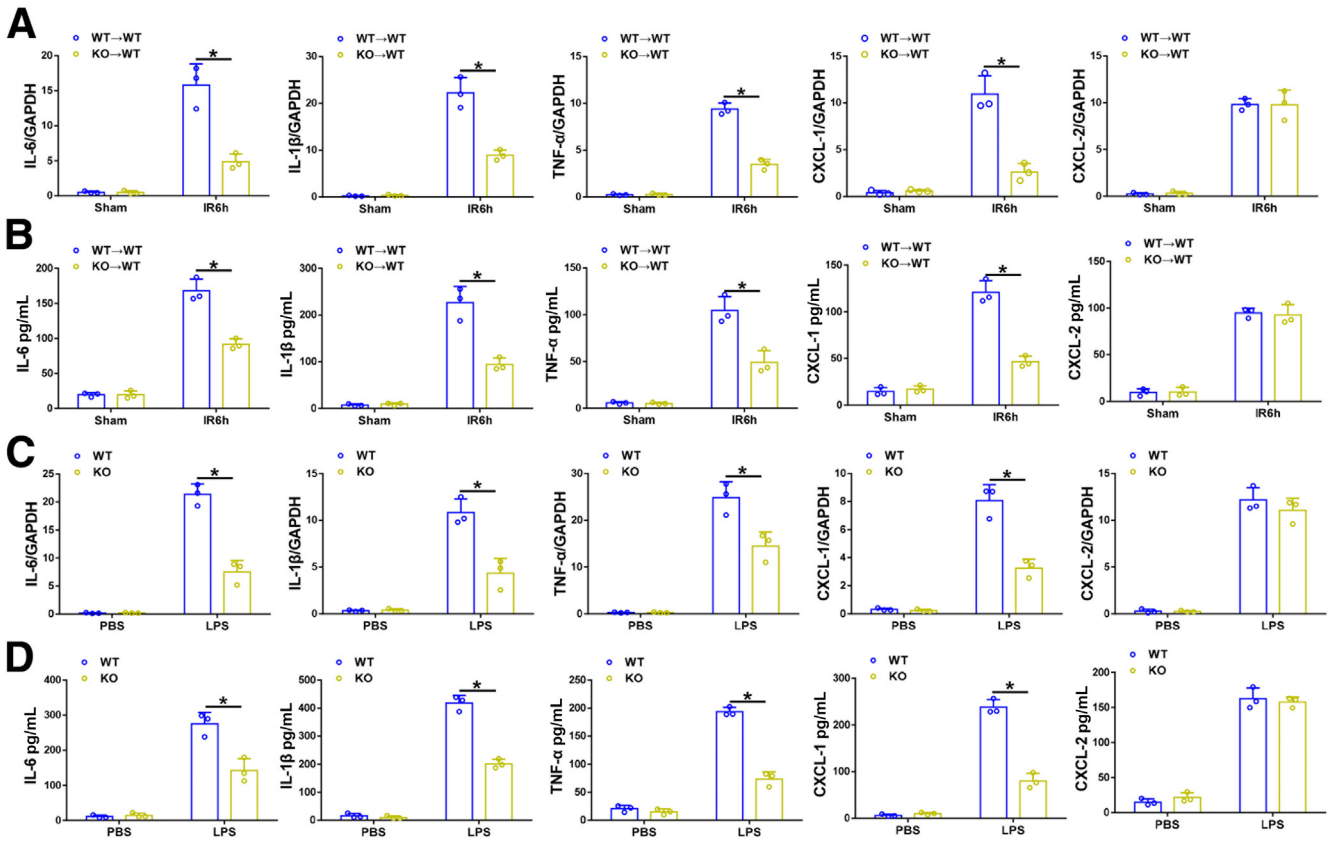

Figure 4. Ninj1-deficient KCs were responsible for decreased expression of proinflammatory cytokines and CXCL-1 both ex vivo and in vitro. WT→WT and KO→WT mice were subjected to 90 minutes of warm ischemia or a sham procedure, and liver tissues were collected at 24 hours after reperfusion. KCs were isolated from livers of each group and were cultured in vitro for 3 hours. The cells and culture supernatant were collected. (*A*) Quantitative RT-PCR analysis of KC inflammatory cytokine and chemokine gene induction (*IL6*, *IL1β*, *TNF-α*, *CXCL-1*, and *CXCL-2*). (*B*) Enzyme-linked immunosorbent assay of inflammatory cytokine and chemokine levels in cells supernatant. KCs isolated from WT and Ninj1 KO mice were stimulated with LPS for 6 hours. The cells and culture supernatant were collected. (*C*) Quantitative RT-PCR analysis of KC inflammatory cytokine and chemokine gene induction (*IL6*, *IL1β*, *TNF-α*, *CXCL-1*, and *CXCL-2*). (*D*) Enzyme-linked immunosorbent assay of inflammatory cytokine and chemokine levels in cell supernatant. All results are representative of at least 2 independent experiments. *$P < .05$. All data are presented as the means ± SD. GAPDH, glyceraldehyde-3-phosphate dehydrogenase; PBS, phosphate-buffered saline.

effectively inhibited DUSP1 and increased p-p38 and p-JNK in KCs isolated from IR-stressed KO→WT livers, but had no effect on KCs isolated from WT→WT livers (Figure 6*A*). The decreased mRNA levels of *IL6*, *IL1β*, *TNF-α*, and *CXCL1* in IR-stressed KO→WT livers were markedly reversed by DUSP1 knockdown, whereas no changes were found in WT→WT livers (Figure 6*B*). Similar results were observed for the serum levels of IL6, IL1β, TNF-α, and CXCL1 (Figure 6*C*). Furthermore, DUSP1-siRNA, but not NS-siRNA, significantly reversed the decreased neutrophil infiltration in KO→WT livers post-IR (Figure 6*D* and *E*). Taken together, IR-induced Ninj1 activation inhibits DUSP1 and subsequently activates the JNK and p38 pathways, leading to intrahepatic inflammation and neutrophil infiltration.

Ninj1 Deficiency Attenuated Liver IR Injury in a DUSP1-Dependent Manner

Next, we investigated the role of Ninj1/DUSP1 signaling in KCs in the regulation of liver IR injury. As shown in Figure 7*A–E*, DUSP1-siRNA–treated WT→WT and KO→WT mice showed similar extents of liver IR injury after 6 hours of reperfusion. However, DUSP1-siRNA treatment significantly reversed the mitigated liver injury in KO→WT mice at 24 hours post-IR, as indicated by increased severity of histologic damage, higher Suzuki scores, and increased levels of AST and ALT (Figure 7*A–E*). In contrast, no changes were observed in WT→WT mice with or without DUSP1-siRNA treatment at 24 hours post-IR. Moreover, decreased hepatocellular apoptosis in IR-stressed KO→WT livers also was abolished by DUSP1 knockdown in KCs, as evaluated by TUNEL staining and levels of apoptosis-related proteins (Figure 7*F–H*). These findings indicate that Ninj1 deficiency protects against liver IR injury by activating DUSP1.

Neutrophil Activity Contributed to Ninj1-Mediated Liver IR Injury In Vivo

We then wondered whether Ninj1 could be a promising therapeutic target for liver IR injury. A Ninj1-neutralizing

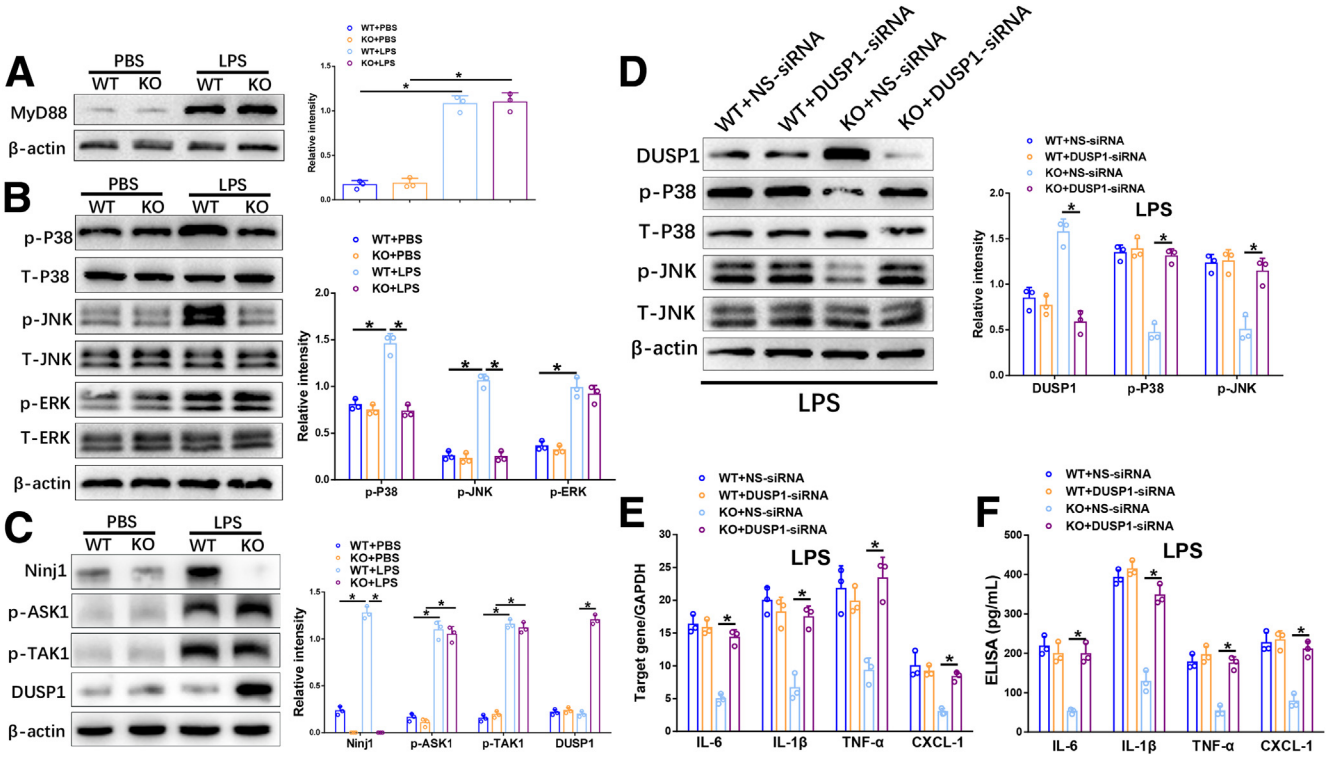

Figure 5. Ninj1 deficiency diminished the inflammatory response in KCs through DUSP1-dependent deactivation of JNK and p38 in vitro. KCs isolated from WT and Ninj1 KO mice were stimulated with LPS for 6 hours. The cells and culture supernatant were collected. (*A*) Western blot analysis of MyD88 and β-actin expression. Relative intensity analyzed by ImageJ software (National Institutes of Health). (*B*) Western blot analysis of p-P38, T-p38, p-JNK, T-JNK, p-ERK, T-ERK, and β-actin expression. Relative intensity analyzed by ImageJ software. (*C*) Western blot analysis of Ninj1, p-ASK1, p-TAK1, DUSP1, and β-actin expression. Relative intensity analyzed by ImageJ software. WT and KO KCs were transfected transiently with DUSP1-siRNA or NS-siRNA followed by LPS stimulation for 6 hours. The cells and culture supernatant were collected. (*D*) Western blot analysis of DUSP1, p-P38, T-p38, p-JNK, T-JNK, and β-actin expression. Relative intensity analyzed by ImageJ software. (*E*) Quantitative RT-PCR analysis of KC inflammatory cytokine and chemokine gene induction (*IL6*, *IL1β*, *TNF-α*, and *CXCL-1*). (*F*) Enzyme-linked immunosorbent assay of inflammatory cytokine and chemokine levels in cell supernatant. All results are representative of at least 2 independent experiments. *$P < .05$. All data are presented as the means ± SD. ELISA, enzyme-linked immunosorbent assay; GAPDH, glyceraldehyde-3-phosphate dehydrogenase; PBS, phosphate-buffered saline. T-p38, Total-p38; T-JNK, Total-JNK; T-ERK, Total ERK.

antibody[21] was used for in vivo studies in WT mice. Blocking Ninj1 significantly protected against liver IR injury as evidenced by reduced necrotic area, decreased Suzuki scores, and decreased serum levels of ALT and AST (Figure 8*A–E*). Based on the aforementioned evidence, we further investigated the role of neutrophil activity in Ninj1-mediated liver IR injury. Sivelestat, a neutrophil elastase inhibitor, was used in both mice and human beings. Our results showed a protective role of sivelestat against liver IR injury in WT→WT mice (Figure 8*F–J*). In contrast, sivelestat treatment had no obvious effects on IR-induced KO→WT mice, suggesting that Ninj1 promotes liver IR injury, partly owing to enhanced neutrophil activity.

For the human study, 10 patients scheduled for partial liver resection with portal occlusion were divided into 2 groups (5/group) according to the presence or absence of preoperative sivelestat treatment. As shown in Figure 8*K*, the serum levels of myeloperoxidase (MPO) 1 day after surgery in the sivelestat group were much lower than those in the control group. Functionally, inhibition of neutrophil elastase activity was accompanied by reduced serum ALT and AST levels 3 days after surgery in the sivelestat group (Figure 8*L* and *M*). These data suggest that enhanced neutrophil activity plays a critical role in liver IR, wherein Ninj1 activation in KCs promotes IR-induced liver injury.

Discussion

This study used bone marrow chimeric mice and showed that Ninj1 deficiency in KCs inhibits IR-induced intrahepatic innate immune responses, decreases neutrophil infiltration, and attenuates liver IR injury. Moreover, it shows that inactivation of P38 and JNK mediated by Ninj1/DUSP1 signaling plays a pivotal role in regulating the IR-induced KC inflammatory response and subsequent liver injury.

Ninj1, a 2-pass transmembrane protein, originally was reported to be up-regulated in neurons and Schwann cells in response to nerve injury and to contribute to axonal growth.[1] In recent years, Ninj1, as an adhesion molecule, has been reported to play diverse roles in many

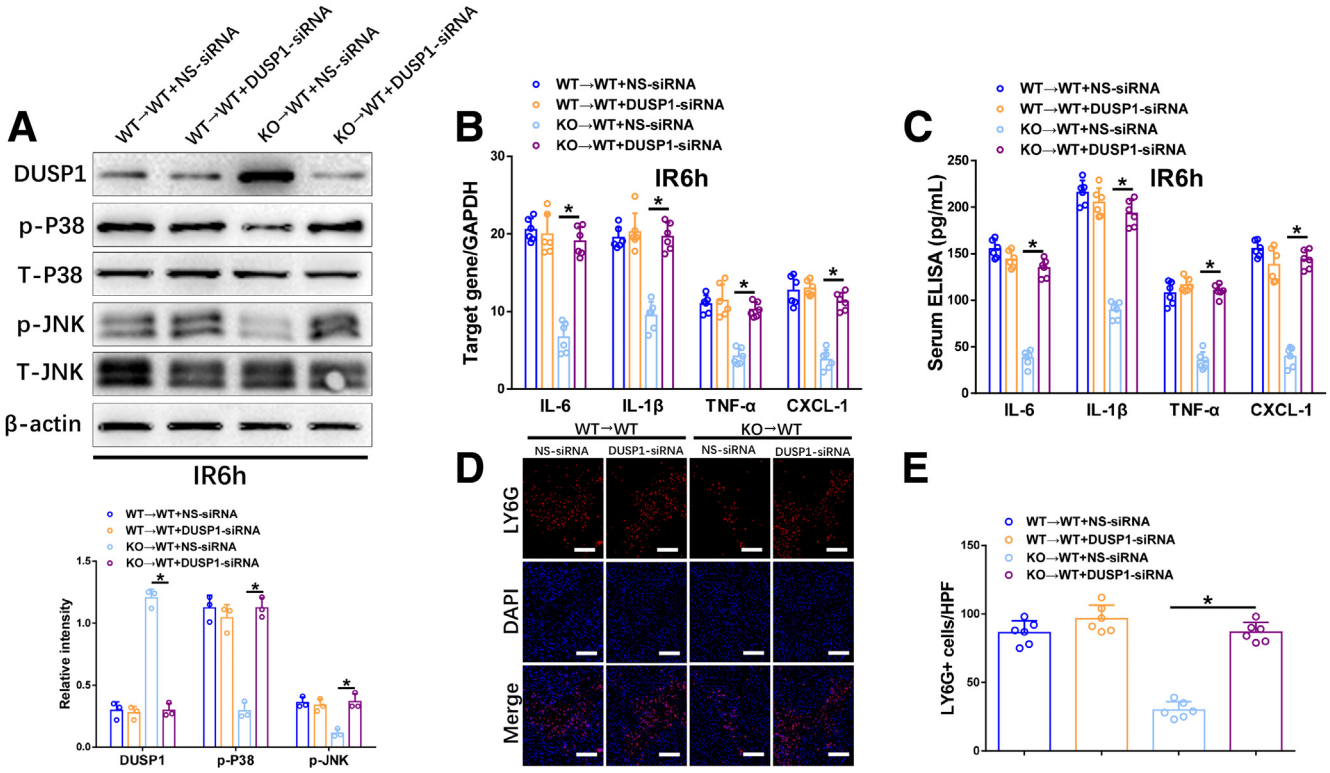

Figure 6. Ninj1 deficiency attenuated IR-induced intrahepatic inflammation and neutrophil infiltration by DUSP1-dependent inhibition of p38 and JNK pathways in vivo. WT→WT and KO→WT mice were treated with either DUSP1-siRNA or NS-siRNA before the onset of liver ischemia, as described in the Materials and Methods section. The liver tissues and blood specimens were collected at 24 hours after reperfusion. (*A*) Western blot analysis of DUSP1, p-P38, T-p38, p-JNK, T-JNK, and β-actin expression. Relative intensity was analyzed by ImageJ software (National Institutes of Health). (*B*) Quantitative RT-PCR analysis of liver inflammatory cytokine and chemokine gene induction (*IL6*, *IL1*β, *TNF-*α, and *CXCL-1*). (*C*) Enzyme-linked immunosorbent assay (ELISA) of inflammatory cytokine and chemokine levels in serum. All results are representative of at least 2 independent experiments. (*D* and *E*) Representative immunofluorescence staining of LY6G (red) and 4',6-diamidino-2-phenylindole dihydrochloride (DAPI) (blue) in livers from each group, quantification of LY6G+ cells per high-power field (HPF), *Scale bar*: 100 μm; n = 6 mice/group. *$P < .05$. All data are presented as the means ± SD. GAPDH, glyceraldehyde-3-phosphate dehydrogenase. T-p38, Total-p38; T-JNK, Total-JNK; LY6G, lymphocyte antigen 6 complex locus g.

pathophysiological processes, especially in the inflammatory context, because of its ability to regulate myeloid cell recruitment.[22,23] However, there are conflicting data regarding the role of Ninj1 in different inflammatory diseases. Ninj1 was found to be up-regulated in blood–brain barrier endothelial cells and on infiltrating myeloid cells in both EAE and human multiple sclerosis lesions in mice correlated with the migration of myeloid cells across the blood–brain barrier; moreover, Ninj1 blockade inhibited the recruitment of inflammatory immune cells and ameliorates the immune response in EAE and multiple sclerosis.[5] Using Ninj1-deficient mice, another study reported that Ninj1 deficiency reduced leukocyte infiltration and attenuated EAE susceptibility in mice.[6] However, a recent study by Jeon et al[24] showed that Ninj1 deficiency increases monocyte recruitment and macrophage accumulation in atherosclerotic lesions as well as enhances macrophage inflammation, resulting in accelerated atherosclerosis. In inflammatory bowel disease, Ninj1 deficiency promotes M1 macrophage polarization and induces microbial imbalance, leading to hypersusceptibility to colitis and severe colitis development.[8] In contrast, Jung et al[9] recently reported a detrimental role of Ninj1 in activating macrophages and exacerbating experimental colitis with no impact on macrophage infiltration. These controversial results indicate that Ninj1 functions diversely under different inflammatory conditions. In the present study, we found that Ninj1 deficiency does not influence IR-induced intrahepatic macrophage recruitment but markedly reduces the levels of inflammatory cytokines and chemokines released by KCs.

An increasing body of evidence indicates that Ninj1 is involved in LPS-induced inflammation and programmed cell death.[23] A direct interaction between LPS and Ninj1 has been reported in LPS-induced macrophage inflammation.[25] Upon LPS stimulation, TLR4, a critical receptor of LPS, activates 2 distinct pathways by MyD88/MyD88 adaptor-like protein and TRIF-related adaptor molecule/TRIF, leading to the activation of downstream signaling involving nuclear factor-κB, MAPK, and interferon-regulated factor transcription factors.[26] Jennewein et al[7] reported that Ninj1 inhibition alleviates LPS-induced macrophage inflammatory responses and leukocyte migration by modulating p38/AP-1

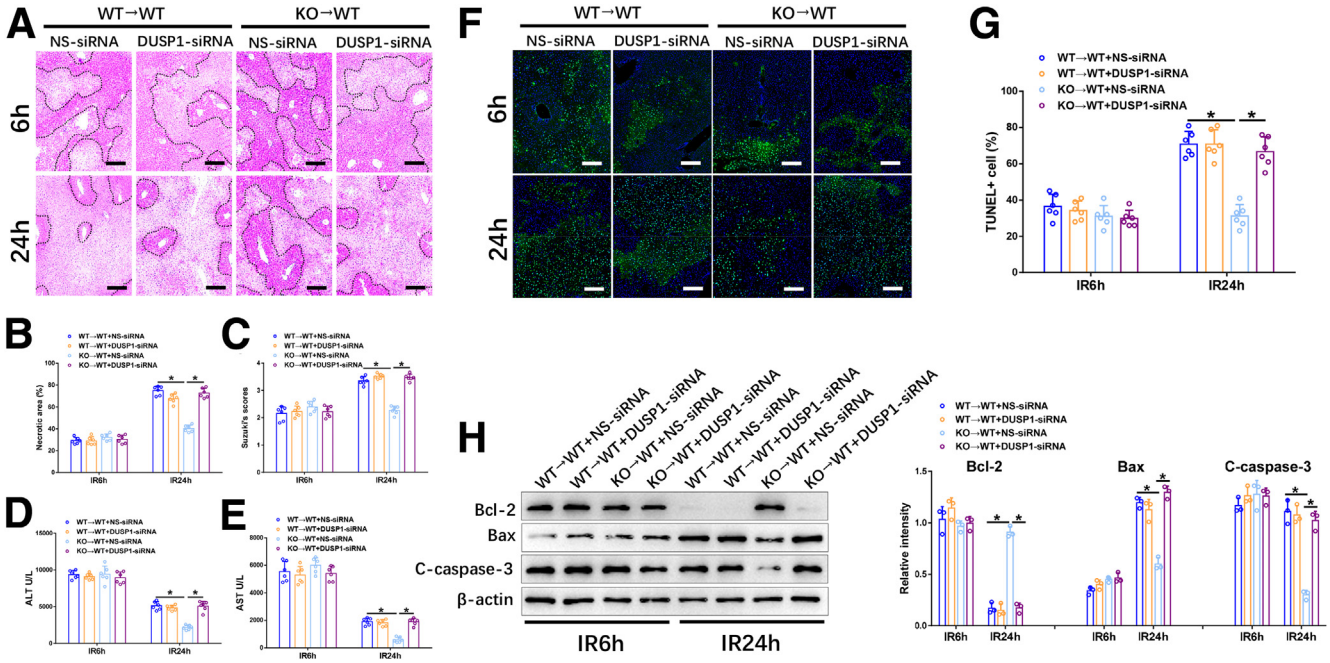

Figure 7. Ninj1 deficiency attenuated liver IR injury in a DUSP1-dependent manner. WT→WT and KO→WT mice were treated with either DUSP1-siRNA or NS-siRNA before the onset of liver ischemia, as described in the Materials and Methods section. The liver tissues and blood specimens were collected at 24 hours after reperfusion. (*A*) Representative H&E staining of ischemic livers from each group for different times. *Scale bar*: 100 μm. (*B*) Necrotic areas in ischemic livers analyzed by ImageJ software (National Institutes of Health). (*C*) Suzuki histologic grading of IR injury. (*D* and *E*) Serum levels of ALT and AST. (*F*) Immunofluorescence staining of TUNEL+ cells in ischemic livers from each group. *Scale bar*: 100 μm. (*G*) Quantification of TUNEL+ cells per high-power field. (*H*) Western blot analysis of Bcl-2, Bax, C-caspase-3, and β-actin expression in livers from each group. Relative intensity was analyzed by ImageJ software. All results are representative of at least 2 independent experiments; n = 6 mice/group. *$P < .05$. All data are presented as the means ± SD. C-caspase-3, Cleaved-caspase-3.

signaling and protects mice against sepsis. A recent study showed that a microRNA-125a-5p mimic can abolish macrophage recruitment and decrease the levels of proinflammatory factors in LPS-inflamed retinas through Ninj1 down-regulation.[27] Interestingly, our ex vivo and in vitro studies have indicated that Ninj1 deficiency mitigates the inflammatory response of KCs by inhibiting p38 and JNK with no impact on MyD88. This motivated us to further explore the molecular mechanism by which Ninj1 regulates p38 and JNK activation.

Mitogen-activated protein kinase kinase kinase/Mitogen-activated protein kinase kinase (MAPKKK/MAPKK) signaling is the classic pathway that modulates MAPK cascades. ASK1 and TAK1 (also known as MAP3K5 and MAP3K7) have been reported to be crucial for activating JNK and p38α cascades. Glutathione S-transferase Mu 2 is an endogenous suppressor that protects against nonalcoholic steatohepatitis progression by suppressing ASK1 phosphorylation and the activation of its downstream JNK/p38 signaling pathway.[15] Tripartite motif-containing 27 plays an important role in regulating liver IR injury by inhibiting TAK1-JNK/p38 signaling.[18] However, our findings in this study showed that Ninj1 deficiency had no impact on activation of ASK1 and TAK1 in LPS-stressed KCs.

DUSP1 has been reported previously to show anti-inflammatory effects in various experimental inflammation models owing to its ability to dephosphorylate MAPK members.[28–31] Several studies have shown that DUSP1 preferentially modulates p38 and JNK to reduce the production of proinflammatory cytokines and chemokines, leading to an attenuated inflammatory response.[19,20,32] Based on these findings, we examined whether Ninj1 regulates p38 and JNK through DUSP1. The results presented in this study confirm the critical role of DUSP1 in Ninj1-mediated deactivation of p38 and JNK in LPS-induced KCs. However, further studies are needed to elucidate the precise mechanisms of interaction between Ninj1 and DUSP1. In addition, as shown in Figure 5*C* and *D*, our findings showed that LPS stimulation significantly increased Ninj1 expression in WT KCs, whereas DUSP1 expression was not changed. However, Ninj1-deficient KCs showed markedly increased DUSP1 expression post-LPS stimulation. These results indicate that Ninj1 inhibited DUSP1 activation in LPS-stimulated KCs. Therefore, although the DUSP1 expression already was suppressed by Ninj1 activation in LPS-stimulated WT KCs, no further effects were found by DUSP1-siRNA.

Studies from our group and others have suggested a critical role for innate immune response–mediated sterile inflammation in liver IR injury.[33,34] Neutrophil infiltration into necrotic areas during the reperfusion period is a hallmark of IR-induced sterile inflammation.[35,36] Our data also indicate that Ninj1 deficiency in KCs markedly restrains IR-induced neutrophil infiltration into the liver with no impact

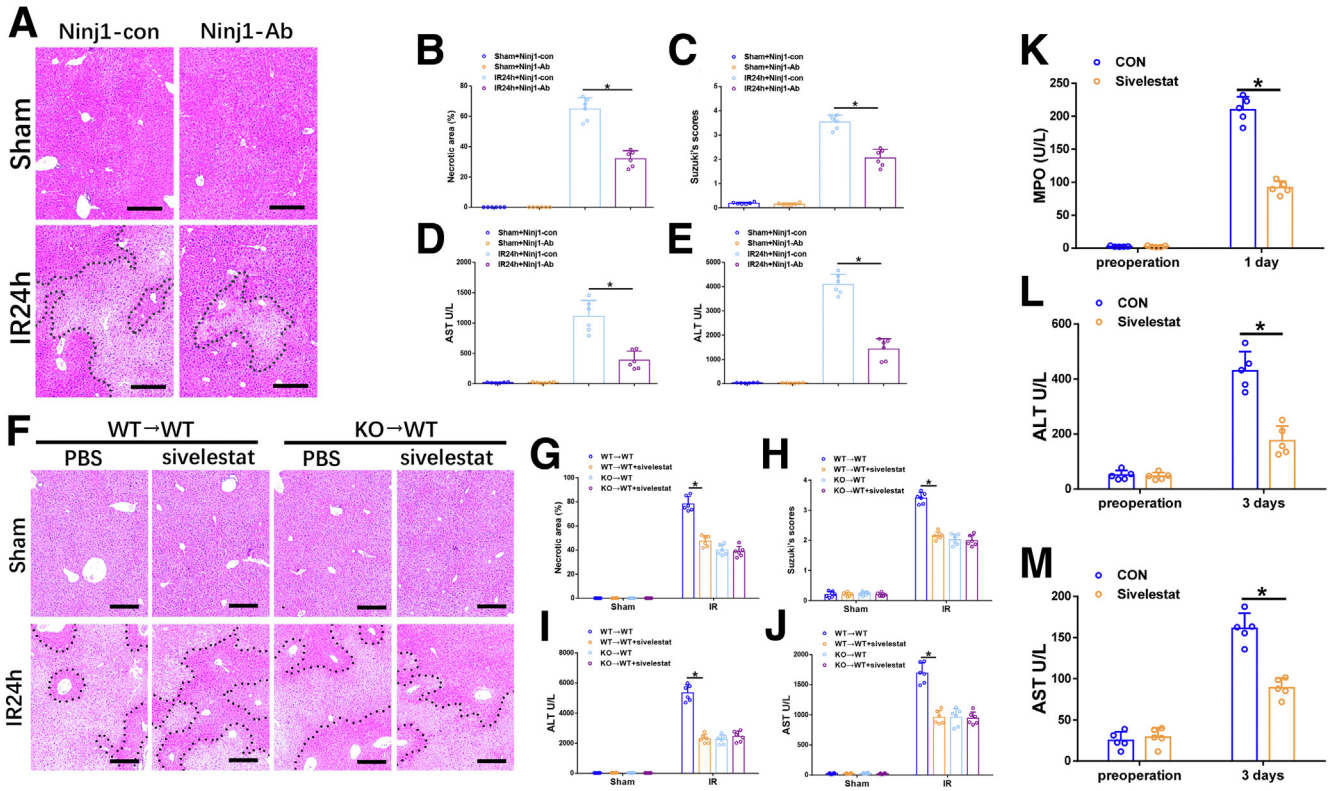

Figure 8. Neutrophil activity contributed to Ninj1-mediated liver IR injury both in mice and human beings. WT mice were administered with Ninj1 neutralizing antibody before the onset of liver ischemia, as described in the Materials and Methods section. (*A*) Representative H&E staining of ischemic livers from each group for different times. *Scale bar*: 100 μm. (*B*) Necrotic areas in ischemic livers analyzed by ImageJ software (National Institutes of Health). (*C*) Suzuki histologic grading of IR injury. (*D* and *E*) Serum levels of ALT and AST. WT→WT and KO→WT mice were treated with sivelestat or phosphate-buffered saline (PBS) before the onset of liver ischemia, as described in the Materials and Methods section. The liver tissues and blood specimens were collected at 24 hours after reperfusion. (*F*) Representative H&E staining of ischemic livers from each group for different times. *Scale bar*: 100 μm. (*G*) Necrotic areas in ischemic livers analyzed by ImageJ software. (*H*) Suzuki histologic grading of IR injury. (*I* and *J*) Serum levels of ALT and AST. Serum specimens were collected from 10 patients (5/group) who received partial liver resection with portal occlusion in the presence or absence of preoperative sivelestat treatment, as described in the Materials and Methods section. (*K–M*) Serum levels of MPO, ALT, and AST. *$P < .05$. All data are presented as the means ± SD. CON, control.

on macrophage recruitment, consistent with previous studies on lung fibrosis and colitis.[9,37] Regarding organ ischemic injury, Ninj1 activation has been reported to increase neutrophil infiltration in the postischemic brain, contributing to aggravated brain injury.[11,12] CXCL1 and CXCL2 are the 2 most important chemoattractants that recruit neutrophils to injured or infected tissues.[38,39] A previous study showed that resident tissue macrophages are a major source of newly synthesized CXCL1 and CXCL2 via different TLR signaling pathways.[13] Interestingly, we found that Ninj1 could influence CXCL1 secretion by KCs both in vivo and in vitro, but not CXCL2, suggesting the presence of distinct modulatory mechanisms underlying the production of these 2 chemokines. In line with a previous study,[40] our results show that CXCL1 alone is sufficient to regulate neutrophil recruitment to the liver.

The CCL family plays an important role in regulating monocyte and lymphocyte migration.[41] CCL5 has been reported to aggravate liver IR injury by chemoattracting macrophages.[42] CCL1, CCL2, and CCL3 also were reported to be important chemoattractants of macrophages and T cells in different diseases.[43–46] Actually, in this study, IR-induced increased levels of CCL family chemokines in our in vivo model were not influenced by Ninj1 deficiency, consistent with the unaltered macrophage recruitment into IR-stressed livers.

Furthermore, in the present study, Ninj1-deficiency–mediated suppression of neutrophil infiltration was suggested to be responsible for mitigating IR-induced liver injury at later time points, consistent with a recent study by Huebener et al, which indicated that High-mobility group box 1 (HMGB1)-receptor for advanced glycation end (RAGE)-induced neutrophil recruitment contributes to subsequent amplification of liver IR injury, 24 hours after reperfusion through neutrophil elastase activity.[47] Sivelestat, an inhibitor of neutrophil elastase, has been reported to protect mice against liver IR injury by inhibiting neutrophil infiltration and suppressing proinflammatory cytokine programs.[48] We also observed a protective effect of sivelestat in IR-induced WT→WT mice, with no obvious effects in

KO→WT mice, indicating a similar mechanism underlying the 2 factors of mitigating liver IR injury. However, whether sivelestat influences neutrophil inflammatory properties via Ninj1 signaling requires further investigation. Interestingly, Hilscher et al[49] recently showed that mechanical forces increased CXCL1 expression in liver sinusoidal endothelial cells, leading to neutrophil recruitment, which is responsible for portal hypertension, whereas sivelestat treatment decreased sinusoidal MPO deposition and depressed portal pressures after partial ligation of the suprahepatic inferior vena cava. Intriguingly, we also found that sivelestat treatment resulted in significantly decreased serum MPO levels and improved liver function in patients who underwent partial hepatectomy with portal triad clamping at 3 days after surgery.

In conclusion, this study shows that Ninj1 in KCs plays a detrimental role in liver IR injury. Ninj1-DUSP1 signaling modulates the proinflammatory response of KCs and influences neutrophil infiltration, partly by regulating CXCL1 production. Overall, our findings provide new insights into the pathogenesis of liver IR injury, and indicate that strategies targeting the Ninj1-DUSP1 signaling axis may be a novel approach to prevent this pathologic process.

Materials and Methods

Patients

Liver tissues were obtained from 10 patients for partial liver resection with portal occlusion. They were divided into 2 groups (5 per group) according to the presence or absence of preoperative sivelestat treatment. Patients in the sivelestat group received 0.2 mg/kg per hour sivelestat intravenously from anesthesia induction to postoperative day 1, while the patients in the control group received the same amount of physiological saline. Serum levels of MPO were measured before and 1 day after the resection, ALT and AST serum levels were analyzed before and 3 days after the resection. Patients were referred to the Affiliated Hospital of Nanjing Medical University after providing informed written consent. All procedures that involved human samples were approved by the Ethics Committee of the Affiliated Hospital of Nanjing Medical University (approval 2020-SRFA-099).

Animals

Male C57BL/6 WT and Ninj1 KO (C57BL/6 background) mice were purchased from Gempharmatech, Co, Ltd (China). Ninj1 KO mice were generated by Clustered regularly interspaced short palindromic repeats (CRISPR)/CRISPR-associated nuclease 9 (Cas9) technology to modify the *Ninj1* gene. Animals were housed under specific pathogen-free conditions, and received humane care according to a protocol (number NMU08-092) approved by the Institutional Animal Care and Use Committee of Nanjing Medical University.

Bone Marrow Transplantation

To delete Kupffer cells, recipient mice were injected intravenously with liposomal clodronate (150 μL). Bone marrow transplantation was performed 24 hours after liposomal clodronate injection. After being lethally irradiated, 5-week-old male WT and KO mice were injected intravenously with 1×10^7 bone marrow cells isolated from 8-week-old male WT or KO mice. Chimeric mice were generated as follows: WT→WT (expressing Ninj1 both in hepatocytes and KCs); and KO→WT (expressing Ninj1 only in hepatocytes). Four weeks after bone marrow transplantation, the chimeras were subjected to a liver IR injury model.

Liver IR Injury Model

Mice were anesthetized with 2.5% isoflurane and an atraumatic clip was used to interrupt the arterial and portal venous blood supply to the cephalad liver lobes for 90 minutes. Sham controls (n = 6) underwent the same procedure, but without vascular occlusion. Then, they were killed after 6 and 24 hours of hepatic tissue reperfusion, and liver and serum samples were collected.

Some mice were administered Ninj1-neutralizing antibody (2.5 μg/20 μL) (BD Biosciences, Franklin Lakes, NJ) or with mouse IgG antibody as control (Ninj1-con) by tail vein injection at 6 hours before the onset of liver ischemia.

Serum Biochemical Measurements

Serum ALT and AST levels were measured with an AU5400 automated chemical analyzer (Olympus, Tokyo, Japan). The serum MPO levels of the patients were measured by an enzyme-linked immunosorbent assay kit according to the manufacture's protocols (Cusabio Technology).

Liver Histopathology

Liver tissues were incubated in 4% paraformaldehyde for at least 24 hours, and then embedded in paraffin. The specimens were sectioned at 4 μm and stained with H&E. The severity of IR injury was scored using the Suzuki criteria on a scale from 0 to 4. No necrosis, congestion/centrilobular ballooning is given a score of 0, while severe congestion and more than 60% lobular necrosis is giver a score of 4.

TUNEL Staining

TUNEL staining of liver tissue sections was performed using a fluorescent detection kit (Roche, Indianapolis, IN) according to the manufacturer's instructions.

Immunofluorescence Staining

Immunofluorescence staining was performed on frozen sections cut into 4-μm slices, blocked and permeated with 3% bovine serum albumin–0.5% Triton X-100 (Sigma) for 30 minutes at room temperature, followed by incubation with rabbit anti-CD11b (1:100, 17800; Cell Signaling Technology, Danvers, MA) and rat anti–Ly-6G (1:200, #88876; Cell Signaling Technology) overnight at 4°C. Nuclei were stained with 4',6-diamidino-2-phenylindole dihydrochloride. Then, slides were washed with phosphate-buffered saline and incubated with horseradish-

peroxidase–conjugated secondary antibodies. Confocal microscopy was performed using an Olympus FV3000 confocal microscopy system.

Cell Culture

Six- to 8-week-old WT and Ninj1 KO mice were anesthetized and the portal vein was canulated under aseptic conditions. The liver was perfused in situ via portal vein with an ethylene glycol-bis(β-aminoethyl ether)-*N,N,N′,N′*-tetraacetic acid solution and digested with 0.075% collagenase type IV (Sigma, St. Louis, MO), perfused liver was filtered through a 40-μm nylon strainer, and centrifuged at 40 $\times$ *g* without brake for 5 minutes. Primary hepatocytes were resuspended in Medium 199 supplemented with 50% Percoll gradient by 200 $\times$ *g* centrifugation and seeded in Dulbecco's modified Eagle medium supplemented with 10% fetal bovine serum. Nonparenchymal cells were suspended in Hank's balanced salt solution and layered onto a 2-layer 25%–50% Percoll (Sigma) gradient in a 50-mL centrifuge tube and centrifuged at 1800 $\times$ *g* at 4ºC for 15 minutes. KCs in the middle layer were collected and allowed to attach to cell culture plates in Dulbecco's modified Eagle medium with 10% fetal bovine serum.

In ex vivo experiments, KCs isolated from IR-stressed KO→WT and WT→WT livers were cultured for 3 hours, and then the cells and supernatants were collected. In in vitro experiments, KCs isolated from WT or KO mice were stimulated with LPS (1 μg/mL; Sigma) for 6 hours.

Quantitative RT-PCR

Total RNA was extracted from tissues and cells with TRIzol reagent (Thermo Fisher Scientific, Carlsbad, CA) followed by isopropyl alcohol precipitation. Quantitative RT-PCR was performed using a 7900 Real-Time PCR System (Applied Biosystems, Foster City, CA) with Fast Start Universal SYBR Green Master Mix (Takara). The expression levels of target genes were normalized against glyceraldehyde-3-phosphate dehydrogenase expression.

Western Blot

Tissue or cellular proteins were extracted and subjected to 10% sodium dodecyl sulfate–polyacrylamide gel electrophoresis and transferred to polyvinylidene difluoride membranes (Bio-Rad, Hercules, CA). Primary antibodies against Ninj1 (PA5-72821; Invitrogen, San Diego, CA), Bcl-2 (#3498; Cell Signaling Technology), Bax (#14796; Cell Signaling Technology), caspase-3 (#9662; Cell Signaling Technology), MyD88 (#4283; Cell Signaling Technology), p-p38 (#4511; Cell Signaling Technology), p38 (#8690; Cell Signaling Technology), p-JNK (#4668; Cell Signaling Technology), JNK (#9252; Cell Signaling Technology), p-ERK (#4370; Cell Signaling Technology), ERK (#4695; Cell Signaling Technology), DUSP1 (#35217; Cell Signaling Technology), p-ASK1 (#3765; Cell Signaling Technology), p-TAK1 (#4531; Cell Signaling Technology), and β-actin (#4970; Cell Signaling Technology) were used and incubated overnight at 4ºC. Bands were detected with Immobilon ECL Ultra Western horseradish peroxidase substrate (Bio-Rad, Hercules, CA), and then images were taken using a Tanon chemiluminescent imaging system.

Enzyme-Linked Immunosorbent Assay

TNF-α, IL6, IL1β, CXCL-1, CXCL-2, CCL1, CCL2, CCL3, and CCL5 in cell culture supernatants or serum was measured by an enzyme-linked immunosorbent assay (eBioscience, San Diego, CA) according to the manufacturer's protocols.

DUSP1 Knockdown

In vitro, 10^6 KCs/well were transfected with mouse DUSP1-siRNA (Thermo Fisher Scientific), or NS-siRNA (Thermo Fisher Scientific) using Lipofectamine 3000 reagent (Thermo Fisher Scientific) according to the manufacturer's protocol. In vivo, siRNA was mixed with mannose-conjugated polymers (Polyplus Transfection, Illkirch, France) at a ratio specified by the manufacturer, and administered by tail vein injection (2 mg/kg siRNA) at 4 hours before the onset of liver ischemia.

Statistical Analysis

The results are presented as the means $\pm$ SD. Multiple group comparisons were performed using 1-way analysis of variance followed by the Bonferroni post hoc test. Statistical analysis was performed using SPSS version 22.0 (SPSS, Inc, Chicago, IL) and an unpaired Student *t* test. $P < .05$ indicated statistical significance.

References

1. Araki T, Milbrandt J. Ninjurin, a novel adhesion molecule, is induced by nerve injury and promotes axonal growth. Neuron 1996;17:353–361.
2. Araki T, Zimonjic DB, Popescu NC, Milbrandt J. Mechanism of homophilic binding mediated by ninjurin, a novel widely expressed adhesion molecule. J Biol Chem 1997;272:21373–21380.
3. Yang HJ, Zhang J, Yan W, et al. Ninjurin 1 has two opposing functions in tumorigenesis in a p53-dependent manner. Proc Natl Acad Sci U S A 2017;114:11500–11505.
4. Toyama T, Sasaki Y, Horimoto M, et al. Ninjurin1 increases p21 expression and induces cellular senescence in human hepatoma cells. J Hepatol 2004;41:637–643.
5. Ifergan I, Kebir H, Terouz S, et al. Role of Ninjurin-1 in the migration of myeloid cells to central nervous system inflammatory lesions. Ann Neurol 2011;70:751–763.
6. Ahn BJ, Le H, Shin MW, et al. Ninjurin1 deficiency attenuates susceptibility of experimental autoimmune encephalomyelitis in mice. J Biol Chem 2014;289:3328–3338.
7. Jennewein C, Sowa R, Faber AC, et al. Contribution of Ninjurin1 to Toll-like receptor 4 signaling and systemic inflammation. Am J Respir Cell Mol Biol 2015;53:656–663.
8. Choi H, Bae SJ, Choi G, et al. Ninjurin1 deficiency aggravates colitis development by promoting M1

macrophage polarization and inducing microbial imbalance. FASEB J 2020;34:8702–8720.
9. Jung HJ, Kang JH, Pak S, et al. Detrimental role of nerve injury-induced protein 1 in myeloid cells under intestinal inflammatory conditions. Int J Mol Sci 2020;21:614.
10. Andersson U, Tracey KJ. HMGB1 is a therapeutic target for sterile inflammation and infection. Annu Rev Immunol 2011;29:139–162.
11. Lee HK, Lee H, Luo L, Lee JK. Induction of nerve injury-induced protein 1 (Ninjurin 1) in myeloid cells in rat brain after transient focal cerebral ischemia. Exp Neurobiol 2016;25:64–74.
12. Lee HK, Kim ID, Lee H, et al. Neuroprotective and anti-inflammatory effects of a dodecamer peptide harboring ninjurin 1 cell adhesion motif in the postischemic brain. Mol Neurobiol 2018;55:6094–6111.
13. De Filippo K, Henderson RB, Laschinger M, Hogg N. Neutrophil chemokines KC and macrophage-inflammatory protein-2 are newly synthesized by tissue macrophages using distinct TLR signaling pathways. J Immunol 2008;180:4308–4315.
14. Arthur JS, Ley SC. Mitogen-activated protein kinases in innate immunity. Nat Rev Immunol 2013;13:679–692.
15. Lan T, Hu Y, Hu F, et al. Hepatocyte glutathione S-transferase mu 2 prevents non-alcoholic steatohepatitis by suppressing ASK1 signaling. J Hepatol 2022;76:407–419.
16. Nakagawa H, Hirata Y, Takeda K, et al. Apoptosis signal-regulating kinase 1 inhibits hepatocarcinogenesis by controlling the tumor-suppressing function of stress-activated mitogen-activated protein kinase. Hepatology 2011;54:185–195.
17. Sakurai H. Targeting of TAK1 in inflammatory disorders and cancer. Trends Pharmacol Sci 2012;33:522–530.
18. Chen SY, Zhang HP, Li J, et al. Tripartite motif-containing 27 attenuates liver ischemia/reperfusion injury by suppressing transforming growth factor beta-activated kinase 1 (TAK1) by TAK1 binding protein 2/3 degradation. Hepatology 2021;73:738–758.
19. Smallie T, Ross EA, Ammit AJ, et al. Dual-specificity phosphatase 1 and tristetraprolin cooperate to regulate macrophage responses to lipopolysaccharide. J Immunol 2015;195:277–288.
20. Escolano A, Martinez-Martinez S, Alfranca A, et al. Specific calcineurin targeting in macrophages confers resistance to inflammation via MKP-1 and p38. EMBO J 2014;33:1117–1133.
21. Yin GN, Choi MJ, Kim WJ, et al. Inhibition of Ninjurin 1 restores erectile function through dual angiogenic and neurotrophic effects in the diabetic mouse. Proc Natl Acad Sci U S A 2014;111:E2731–E2740.
22. Lee HJ, Ahn BJ, Shin MW, et al. Ninjurin1: a potential adhesion molecule and its role in inflammation and tissue remodeling. Mol Cells 2010;29:223–227.
23. Newton K, Dixit VM, Kayagaki N. Dying cells fan the flames of inflammation. Science 2021;374:1076–1080.
24. Jeon S, Kim TK, Jeong SJ, et al. Anti-inflammatory actions of soluble Ninjurin-1 ameliorate atherosclerosis. Circulation 2020;142:1736–1751.
25. Shin MW, Bae SJ, Wee HJ, et al. Ninjurin1 regulates lipopolysaccharide-induced inflammation through direct binding. Int J Oncol 2016;48:821–828.
26. Akira S, Takeda K. Toll-like receptor signalling. Nat Rev Immunol 2004;4:499–511.
27. Hwang SJ, Ahn BJ, Shin MW, et al. miR-125a-5p attenuates macrophage-mediated vascular dysfunction by targeting Ninjurin1. Cell Death Differ 2022;29:1199–1210.
28. Manetsch M, Che W, Seidel P, et al. MKP-1: a negative feedback effector that represses MAPK-mediated pro-inflammatory signaling pathways and cytokine secretion in human airway smooth muscle cells. Cell Signal 2012;24:907–913.
29. Lang R, Hammer M, Mages J. DUSP meet immunology: dual specificity MAPK phosphatases in control of the inflammatory response. J Immunol 2006;177:7497–7504.
30. Vandevyver S, Dejager L, Van Bogaert T, et al. Glucocorticoid receptor dimerization induces MKP1 to protect against TNF-induced inflammation. J Clin Invest 2012;122:2130–2140.
31. Zhang Y, Leung DY, Richers BN, et al. Vitamin D inhibits monocyte/macrophage proinflammatory cytokine production by targeting MAPK phosphatase-1. J Immunol 2012;188:2127–2135.
32. Frazier WJ, Wang X, Wancket LM, et al. Increased inflammation, impaired bacterial clearance, and metabolic disruption after gram-negative sepsis in Mkp-1-deficient mice. J Immunol 2009;183:7411–7419.
33. Zhou H, Zhou S, Shi Y, et al. TGR5/cathepsin E signaling regulates macrophage innate immune activation in liver ischemia and reperfusion injury. Am J Transplant 2021;21:1453–1464.
34. Kadono K, Kageyama S, Nakamura K, et al. Myeloid Ikaros-SIRT1 signaling axis regulates hepatic inflammation and pyroptosis in ischemia-stressed mouse and human liver. J Hepatol 2022;76:896–909.
35. Oliveira THC, Marques PE, Proost P, Teixeira MMM. Neutrophils: a cornerstone of liver ischemia and reperfusion injury. Lab Invest 2018;98:51–62.
36. Fan Q, Tao R, Zhang H, et al. Dectin-1 contributes to myocardial ischemia/reperfusion injury by regulating macrophage polarization and neutrophil infiltration. Circulation 2019;139:663–678.
37. Choi S, Woo JK, Jang YS, et al. Ninjurin1 plays a crucial role in pulmonary fibrosis by promoting interaction between macrophages and alveolar epithelial cells. Sci Rep 2018;8:17542.
38. Drummond RA, Swamydas M, Oikonomou V, et al. CARD9(+) microglia promote antifungal immunity via IL-1beta- and CXCL1-mediated neutrophil recruitment. Nat Immunol 2019;20:559–570.
39. De Filippo K, Dudeck A, Hasenberg M, et al. Mast cell and macrophage chemokines CXCL1/CXCL2 control the early stage of neutrophil recruitment during tissue inflammation. Blood 2013;121:4930–4937.
40. Hwang S, He Y, Xiang X, et al. Interleukin-22 ameliorates neutrophil-driven nonalcoholic steatohepatitis through multiple targets. Hepatology 2020;72:412–429.

41. Griffith JW, Sokol CL, Luster AD. Chemokines and chemokine receptors: positioning cells for host defense and immunity. Annu Rev Immunol 2014;32:659–702.
42. Lee CM, Peng HH, Yang P, et al. C-C chemokine ligand-5 is critical for facilitating macrophage infiltration in the early phase of liver ischemia/reperfusion injury. Sci Rep 2017;7:3698.
43. Heymann F, Hammerich L, Storch D, et al. Hepatic macrophage migration and differentiation critical for liver fibrosis is mediated by the chemokine receptor C-C motif chemokine receptor 8 in mice. Hepatology 2012; 55:898–909.
44. Zen Y, Liberal R, Nakanuma Y, et al. Possible involvement of CCL1-CCR8 interaction in lymphocytic recruitment in IgG4-related sclerosing cholangitis. J Hepatol 2013;59:1059–1064.
45. Li X, Yao W, Yuan Y, et al. Targeting of tumour-infiltrating macrophages via CCL2/CCR2 signalling as a therapeutic strategy against hepatocellular carcinoma. Gut 2017; 66:157–167.
46. Xu L, Chen Y, Nagashimada M, et al. CC chemokine ligand 3 deficiency ameliorates diet-induced steatohepatitis by regulating liver macrophage recruitment and M1/M2 status in mice. Metabolism 2021;125:154914.
47. Huebener P, Pradere JP, Hernandez C, et al. The HMGB1/RAGE axis triggers neutrophil-mediated injury amplification following necrosis. J Clin Invest 2019; 130:1802.
48. Uchida Y, Freitas MC, Zhao D, et al. The protective function of neutrophil elastase inhibitor in liver ischemia/reperfusion injury. Transplantation 2010;89:1050–1056.
49. Hilscher MB, Sehrawat T, Arab JP, et al. Mechanical stretch increases expression of CXCL1 in liver sinusoidal endothelial cells to recruit neutrophils, generate sinusoidal microthombi, and promote portal hypertension. Gastroenterology 2019;157:193–209 e9.

Received July 17, 2022. Accepted January 23, 2023.

Correspondence
Address correspondence to: Shun Zhou, MD, PhD, or Xun Wang, MD, PhD, Hepatobiliary Center, The First Affiliated Hospital, Nanjing Medical University, 300 Guangzhou Road, Nanjing 210000, People's Republic of China. e-mail: hand2399@njmu.edu.cn or wangxun@njmu.edu.cn.

CRediT Authorship Contributions
Shun Zhou, PhD, MD (Conceptualization: Lead; Funding acquisition: Lead; Project administration: Lead; Supervision: Lead; Writing – original draft: Lead; Writing – review & editing: Lead)
Yuanchang Hu (Data curation: Lead; Investigation: Lead; Writing – original draft: Lead; Writing – review & editing: Lead)
Feng Zhan (Data curation: Equal; Investigation: Equal)
Yong Wang (Writing – original draft: Equal; Writing – review & editing: Equal)
Dong Wang (Data curation: Supporting)
Hao Lu (Data curation: Supporting; Methodology: Supporting)
Chen Wu (Investigation: Supporting)
Yongxiang Xia (Funding acquisition: Equal; Supervision: Supporting)
Lijuan Meng (Methodology: Supporting)
Feng Zhang (Data curation: Supporting)
Xun Wang (Conceptualization: Equal; Project administration: Equal)

Conflicts of interest
The authors disclose no conflicts.

Funding
This work was supported by grants from the National Nature Science Foundation of China (82103125, 82070676).

Data availability statement
The data that support the findings of this study are available on request from the corresponding author.